Biosensors and Bioelectronics 79 (2016) 98–107

Contents lists available at ScienceDirect

Biosensors and Bioelectronics

journal homepage: www.elsevier.com/locate/bios

Sensitive biomolecule detection in lateral flow assay with a portable temperature–humidity control device

Jane Ru Choi [a,b,c], Jie Hu [b,c], Shangsheng Feng [b,d,e], Wan Abu Bakar Wan Abas [a], Belinda Pingguan-Murphy [a,*], Feng Xu [b,c,**]

[a] Department of Biomedical Engineering, Faculty of Engineering, University of Malaya, Lembah Pantai, 50603 Kuala Lumpur, Malaysia
[b] The Key Laboratory of Biomedical Information Engineering of Ministry of Education, School of Life Science and Technology, Xi'an Jiaotong University, Xi'an 710049, PR China
[c] Bioinspired Engineering and Biomechanics Center (BEBC), Xi'an Jiaotong University, Xi'an 710049, PR China
[d] MOE Key Laboratory for Multifunctional Materials and Structures (LMMS), School of Aerospace, Xi'an Jiaotong University, Xi'an, PR China
[e] State Key Laboratory of Mechanical Structure Strength and Vibration, School of Aerospace, Xi'an Jiaotong University, Xi'an, PR China

ARTICLE INFO

Article history:
Received 31 July 2015
Received in revised form
30 November 2015
Accepted 4 December 2015
Available online 7 December 2015

Keywords:
LFA
POC
Nucleic acid hybridization
Antigen–antibody interaction
Temperature
RH
Portable temperature–humidity control device

ABSTRACT

Lateral flow assays (LFAs) have currently attracted broad interest for point-of-care (POC) diagnostics, but their application has been restricted by poor quantification and limited sensitivity. While the former has been currently solved to some extent by the development of handheld or smartphone-based readers, the latter has not been addressed fully, particularly the potential influences of environmental conditions (e.g., temperature and relative humidity (RH)), which have not yet received serious attention. The present study reports the use of a portable temperature–humidity control device to provide an optimum environmental requirement for sensitivity improvement in LFAs, followed by quantification by using a smartphone. We found that a RH beyond 60% with temperatures of 55–60 °C and 37–40 °C produced optimum nucleic acid hybridization and antigen–antibody interaction in LFAs, respectively representing a 10-fold and 3-fold signal enhancement over ambient conditions (25 °C, 60% RH). We envision that in the future the portable device could be coupled with a fully integrated paper-based sample-to-answer biosensor for sensitive detection of various target analytes in POC settings.

1. Introduction

With the rapidly increasing incidence of infectious diseases (e.g., Ebola, dengue, malaria, human immunodeficiency virus (HIV) and influenza) owing to globalization, limited access to medical services in developing countries has become a major challenge (Laursen, 2012; McNerney and Daley, 2011). To address this issue effectively, a robust system is required to bring accurate diagnostic assays to the point of care (POC). This could greatly simplify the existing laboratory-based assays (i.e., quantitative real-time polymerase chain reaction (qRT-PCR) and enzyme-linked immunosorbent assay (ELISA)) as well as reducing the cost and time demands they bring about, especially in resource-limited settings, where most diseases exist (Burke and Gorodetsky, 2012; Han et al., 2014; Sackmann et al., 2014). Today, the use of a paper-based platform represents a promise of a simple, portable, cost-effective, and user-friendly POC diagnostic tool, which holds a great potential as an alternative to the conventional laboratory techniques (Choi et al., 2015; Song et al., 2012). Recent studies have focused on the use of lateral flow assay (LFA) for accurate POC diagnostics (Blažková et al., 2009; Hu et al., 2013; Wang et al., 2013). These assays normally involve hybridization of a single stranded-target analyte (RNA or DNA) with a complementary probe to form a double-stranded nucleic acid, or binding between antigen (Ag) and antibody (Ab) to form an Ag-Ab complex, which produces a colorimetric, fluorescent or chemiluminescent signal (Cate et al., 2014; Martinez, 2011). However, to date, the main limitations of LFA are the difficulties in quantification and lack of sensitivity (Feng et al., 2015; Hu et al., 2014).

Several efforts have been made to address these limitations. To achieve quantification, researchers have developed a variety of handheld or smartphone-based readers to quantify the LFA results (Mudanyali et al., 2012). As for the sensitivity improvement, various techniques have been developed through probe-based signal enhancement (Hu et al., 2013), enzyme-based signal enhancement (He et al., 2011), thermal contrast (Qin et al., 2012), or fluidic

* Corresponding author.
** Corresponding author at: Bioinspired Engineering and Biomechanics Center (BEBC), Xi'an Jiaotong University, Xi'an 710049, PR China.
E-mail addresses: bpingguan@um.edu.my (B. Pingguan-Murphy), fengxu@mail.xjtu.edu.cn (F. Xu).

http://dx.doi.org/10.1016/j.bios.2015.12.005
0956-5663/

control (Parolo et al., 2013; Rivas et al., 2014). However, the sensitivity of LFA might be significantly affected by the environmental conditions, which have been overlooked in most studies. Accumulating evidence has shown that environmental factors (e.g., temperature and relative humidity (RH)) may have a significant influence on biomolecular reactions (Barry and DeMille, 2012; De Roy et al., 2013; Wu et al., 2014), including nucleic acid hybridization (Zhang et al., 2012) and Ag–Ab interaction (Reverberi and Reverberi, 2007). Further, RH may also influence the assay readout by affecting the fluid wicking rate in the paper, which may in turn affect the sensitivity of paper-based assays (Giokas et al., 2014; Lutz et al., 2013; Renault et al., 2013; Rivas et al., 2014). As LFAs are intended for field application, they may be affected by user's environmental conditions (e.g., extremely hot or cold, and dry or wet environments) more than in a typical controlled laboratory. For instance, the temperature and RH of well-known dengue endemic area, Malaysia, is in the range of 25–37 °C and 70–90% RH, respectively, which may not produce an optimum assay outcome. Therefore, effective monitoring and control of environmental factors plays an important role in maintaining optimum conditions for biomolecular reactions, and in turn enhancing the analytical sensitivity of the current LFA. Several studies have investigated the stability of LFA in different environmental conditions (Chien et al., 2006; Johnson et al., 2005). However, the optimum environmental requirement for sensitivity enhancement in LFA for nucleic acid or antigen/antibody detection has not been explored yet.

The present study reports the use of a portable temperature–humidity control device to provide an optimum environmental requirement for sensitivity improvement in LFAs, followed by quantification of multiple types of targets (DNA or protein) by using a smartphone. Interestingly, in DNA detection, temperatures between 55–60 °C (representing the annealing temperature in PCR) provides the maximal DNA hybridization signal, without significantly affecting the shape of the paper (e.g., deformation), whereas an RH beyond 60% could effectively facilitate the fluid to completely wick through the paper to produce the desired signal. With optimum experimental conditions (55 °C, >60% RH) our lateral flow test strip was able to improve the sensitivity of almost 10-fold compared to that achieved at ambient conditions (25 °C, 60% RH), using dengue viral DNA and HIV DNA as model analytes. We have also successfully shown the optimum Ab–Ag interaction at 37–40 °C by using this simple test strip. Given that precise temperature and humidity control is technically challenging outside the laboratory, we developed a portable temperature–humidity control device to achieve optimum LFA performance in a POC setting (Fig. 1). We envision that in the future, the integration of a fully integrated paper-based sample-to-answer biosensor into this portable device offers great potential for sensitive detection of various target analytes in resource-poor settings.

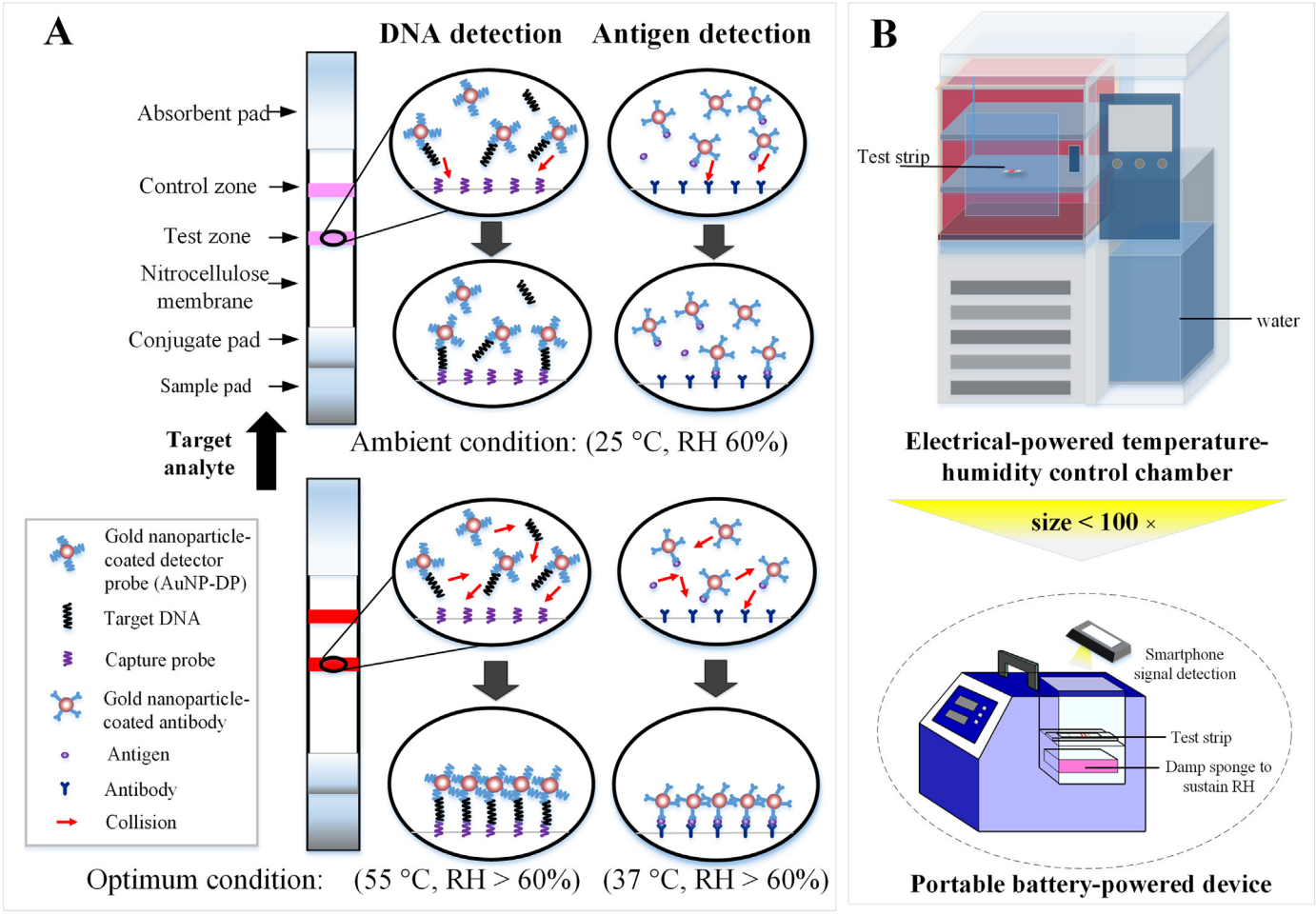

Fig. 1. Schematic of sensitive biomolecule detection in lateral flow assay at optimum temperature and humidity. To rapidly and accurately detect the target analytes by LFA at optimum conditions (55 °C for nucleic acid detection or 37 °C for antigen detection, >60% RH) in the remote settings, a small and portable temperature–humidity control device was developed, coupled with a smartphone signal detection, to substitute the large and complex commercial temperature–humidity control device. The optimum temperature of 55 °C and 37 °C enhanced the binding of the DNA–DNA and antigen–antibody, respectively, producing the enhanced LFA signal than that of 25 °C. RH: relative humidity.

2. Material and methods

2.1. Preparation of gold nanoparticles (AuNP) and AuNP-DP (detector probes) conjugates

Gold nanoparticle (AuNP) with diameter of 13 ± 3 nm were prepared according to the previously published protocol (Hu et al., 2013). In a 250 mL round-bottom flask, 4.5 mL of 1% tri-sodium citrate and 1.2 mL of 0.825% chloroauric acid was added to 100 mL-boiled ultrapure water. The solution turned from yellow to purple and finally turned wine-red in 2 min. The solution was used to prepare AuNP-DP conjugates. Both AuNP and AuNP-DP conjugates were characterized by UV/Vis spectrophotometry and TEM (TEM, JEM-2100F).

About 100 μM of thiolated oligonucleotide (detector probe, DP) was used to conjugate with AuNPs, with the ratio of the volume of gold nanoparticle to oligonucleotide 160:1. The 24.1 nmol oligonucleotide was activated before the conjugation, by mixing with 39 μL of 500 mM acetate buffer (pH 4.76), 8 μL of 10 nM tris(2-carboxyethyl)phosphine (TCEP) and 194 μL of distilled water to achieve a final concentration of 100 μM. After 24 h, 1% sodium dodecyl sulphate (SDS) and 2 M NaCl were added to the solution to reach a final concentration of 0.01% SDS and 0.16 M NaCl, respectively. Following the centrifugation at 10,000 rpm, the pellet was suspended in 1 mL eluent buffer, consisting of 5% BSA, 0.25% Tween 20, 10% sucrose and 20 nM Na_3PO_4. The gold nanoparticle-detector probe conjugates (AuNP-DP) with the concentration of 3 nM were characterized by visible colour changes from wine red to dark red (Supplementary Fig. 1A), a slight shift of the absorbance values (6 nm) in ultraviolet-visible (UV/Vis) spectrophotometry (Supplementary Fig. 1B) and AuNP-DP aggregates formation in transmission electron microscopy (TEM) as compared to AuNP (Supplementary Fig. 1C), with the particle size of 13 nm (Supplementary Fig. 1D).

2.2. Fabrication of lateral flow test strip

The lateral flow test strip is made up of a nitrocellulose membrane (30 cm × 2.0 cm × 0.01 cm) (HFB 18002, Millipore, USA), a sample pad (30 cm × 1.2 cm × 0.05 cm) (H-8, Jiening, China), a conjugate pad (30 cm × 0.8 cm × 0.05 cm) (Pall 8964, Saint Germain-en-Laye, France) and an absorbent pad (30 cm × 2.5 cm × 0.1 cm) (H-1, Jiening, China), mounted on a PVC backing pad (30 cm × 6.0 cm × 0.02 cm) (J-B6, Jiening, China). By using Matrix™ 2360 Programmable Shear, the assembled pads were then cut into a large number of strips with 6 cm length and 0.25 cm width. About 0.5 μL of 100 μM control probe were dispensed on control zone, whereas the equal amounts of each capture probe were mixed before 0.5 μL of 100 μM mixture being dispensed onto a test zone. Streptavidin was used to combine with the biotinylated DNA probes to facilitate the immobilization of DNA probes on the nitrocellulose membrane. The capture probe was prepared by mixing the capture probe in powder form (21.6 nmol) with 165 μL of 2 mg/mL streptavidin-PBS solution (5.5 nmol of streptavidin) and 29 μL of PBS, followed by 22 μL of ethanol after the 1 h incubation, to reach the final concentration of 100 μM. After adding 10 μL AuNP-DNA conjugates to each test strip, they were then dried at 37 °C for 2 h.

2.3. Optimization, sensitivity and specificity assays at ambient condition

In nucleic acid testing (NAT), RNA viruses such as Dengue viruses are normally extracted, followed by the process of reverse-transcription and amplification, and finally target DNA detection (Dauner et al., 2015; Teoh et al., 2015). As DNA is normally the final analyte in NAT, we used synthetic Dengue viral DNAs as model analytes for proof-of-principle investigation of the effects of environmental condition on sensitivity of LFA by using the portable temperature–humidity control device. The test strip was able to detect four serotypes of virus DNAs (dengue viruses, DENV 1–4), which allowed multiple analyte detection in a single test strip. All sequences used in the study were obtained from Sangon Biotechnology Co., Ltd. (Shanghai, China) (Supplementary Table 1). The highly conserved regions of the dengue virus genome were selected as capture and detector probes (Stubbs et al., 2011). About 20, 24, 23 and 22 bp of capture probes are hybridized with one side of target DENV 1, 2, 3 and 4 sequence respectively, with 21 bp of detector probes hybridizing with another side of each target DENV sequence.

Various concentration of capture probes (50 μM, 100 μM and 500 μM), AuNP-DP (3 nM, 6 nM and 9 nM) and SSC buffer (2 ×, 4 ×, 6 × and 8 ×) were prepared to study their effects on the test strip at ambient condition (25 °C, 60% RH). The SSC buffer used in this study was diluted from the commercial SSC buffer 20 × (Sigma-Aldrich). The desired concentration of target DNA was prepared by dilution with SSC buffer. Subsequently, 50 μL of target DNA solution was added onto the sample pad. The test strip was then tested and the colour formation in the test zone was observed. At the end of each assay, images of all the test zones were captured with a smartphone, and the colour intensities were converted to optical density with Image Pro Plus 6.0 software (Media cybernetics. Inc., Bethesda, MD). The optical density (OD) presented in the graph represents the difference between OD of a certain target concentration and OD of negative control (0 nM). The OD corresponding to the intensity of the test zone presented in different graph might be different due to the different set of negative control used in different group of experiment. A sensitivity assay was performed to determine the limit of detection at ambient condition with eight different target concentrations.

2.4. LFA at various temperature and relative humidity (RH)

To study the effect of RH on fluid flow, the shape of test strip and DNA hybridization signal, the assay was performed at 40%, 50%, 60%, 70%, 80% and 90% RH using 10 nM of target. With the optimum RH, the assay was performed at different temperatures, 10, 20, 30, 40, 50, 55, 60, 65 and 70 °C. All data was collected in 10 min per condition. A sensitivity assay was performed for detection of DNA of DENV at optimum temperature and RH.

For an additional proof-of-principle, the sensitivity assay was repeated with DENV and another two types of target analytes, HIV (DNA) and C-reactive protein (Ag) by using our temperature–humidity control device. The same procedure of strip preparation was repeated for HIV DNA. As for the testing of C-reactive protein, the test strips containing Anti-mouse (goat) IgG polyclonal antibody and anti-CRP antibody, and CRP antigen were given by Fapon's Laboratory. Briefly, AuNPs with an average diameter of 30 nm were adjusted to pH 8.0 with 5 μL of 0.2 M potassium carbonate (K_2CO_3). Then about 150 μl anti-CRP antibody (12 μg /mL) was added to 1 mL AuNP and was incubated at room temperature for 30 min. About 10% BSA was then added to block the unconjugated surfaces of gold nanoparticles to obtain a final concentration of 0.1%. The supernatant was removed after 10 min of centrifugation at 14,000 × *g*. The pellet was resuspended in 1 mL eluent buffer containing 0.85% Tris, 1% BSA, 20% sucrose and 5% trehalose.

Goat anti-mouse IgG polyclonal antibody and anti-CRP antibody were diluted with coating buffer (2% trehalose in 0.01 M PBS) to 1 mg/mL. The anti-mouse IgG polyclonal antibody and anti-CRP antibody were dispensed onto the nitrocellulose membrane to create both control and test zones, respectively using reagent-

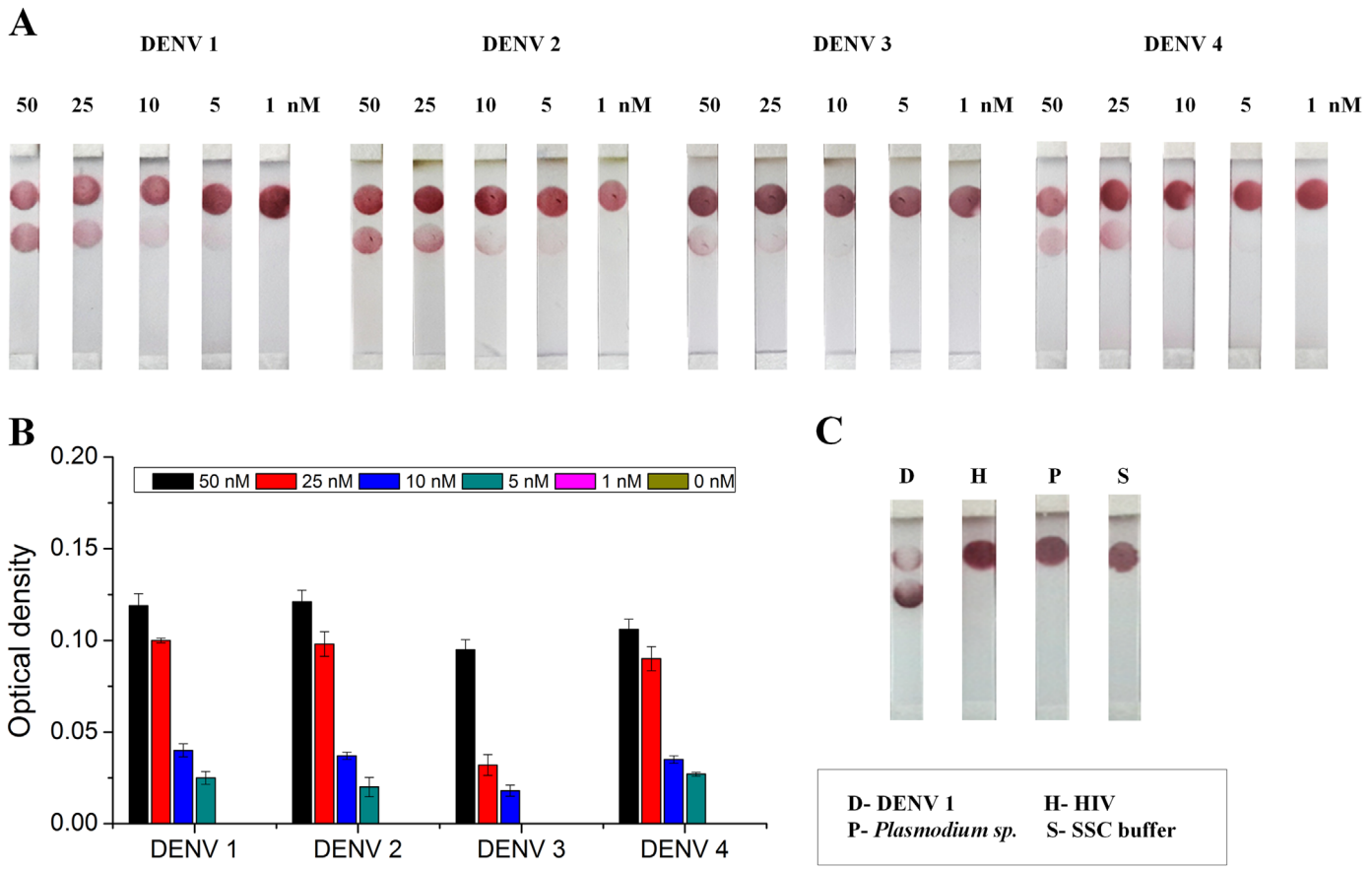

Fig. 2. Sensitivity and specificity assay. (A and B) The detection limit of the asssay was as low as 5–10 nM, as indicated by the detection limit of as low as 5 nM achieved by DENV 1, 2 and 4, and the detection limit of 10 nM achieved by DENV 3. (C) The assay was highly specific as indicated by the only positive result shown in the presence of DENV, whereas the negative result shown in the presence of HIV, Plasmodium sp. and SSC buffer.

dispensing module HM3030 (Shanghai Kinbio Tech, China). AuNP-anti CRP antibody was added onto the conjugate pad. All materials including nitrocellulose membrane, absorbent pad, conjugate pad and sample pad were mounted onto a backing pad. The as-assembled pads were then cut into strips by Programmable shear ZQ4000 (Shanghai Kinbio Tech, China).

2.5. Statistical analysis

Statistical analysis was performed using One-Way ANOVA with Tukey post-hoc test to compare the data among different groups in optimization assays and temperature and humidity assays. Data were expressed as mean ± standard error of the mean (SEM) of three independent experiments ($n=3$). $p<0.05$ was reported as statistically significant.

3. Results and discussion

3.1. The working principle of lateral flow assay in a temperature–humidity-controlled manner

LFAs are commonly performed based on nucleic acid hybridization or Ag–Ab reactions. Both test strips are made up of a nitrocellulose membrane containing a test zone and a control zone, a sample pad, a conjugate pad deposited with AuNP-DP, an absorbent pad to facilitate the fluid flow and a backing pad as a support of the strip. In nucleic acid detection, the target DNAs are allowed to bind to the AuNP-DP, forming AuNP-DP-target DNA complexes, which in turn interact with the capture probe at the test zone to produce a red signal observable by the naked eyes. The excess AuNP-DP binds to the control probe at the control zone. In Ag detection, the Ag binds to the AuNP-Ab, forms complexes, and binds to the immobilized Ab at the test zone, whereas the control zone with immobilized anti-rabbit Ab serves as a control. In this study, we found that optimum RH (> 60%) facilitates complete fluid flow in paper, whereas the temperatures of 55–60 °C and 37–40 °C increase molecular kinetics and strengthens the chemical bond of DNA-DNA and Ag–Ab (Fig. 1A), respectively, which are in agreement with the existing theories (Reske et al., 2007; Reverberi and Reverberi, 2007; Vlachou et al., 2010) as briefly discussed in the following sections. As a result, optimum conditions were able to enhance the analytical sensitivity in LFAs. With this principle, we developed a small and portable battery-powered temperature–humidity control device for use in remote settings as a substitute for the commonly used high-cost and large-sized temperature–humidity control device, which requires an external electrical power supply (Fig. 1B).

3.2. Assay optimization

To perform the LFA with an optimum concentration of reagents, we first optimized the concentration of the capture probe, AuNP-DP, and the SSC buffer required in the assay at ambient conditions (25 °C, 60% RH). To determine the optimum concentration of the capture probe, we performed the assay using 50, 100 and 500 μM of capture probe. We found that the optical density of the test zone was significantly increased with 100 μM capture probe as compared to 50 μM ($p<0.05$). The result indicates that 100 μM capture probe was able to capture more AuNP-DP–DNA complex, hence

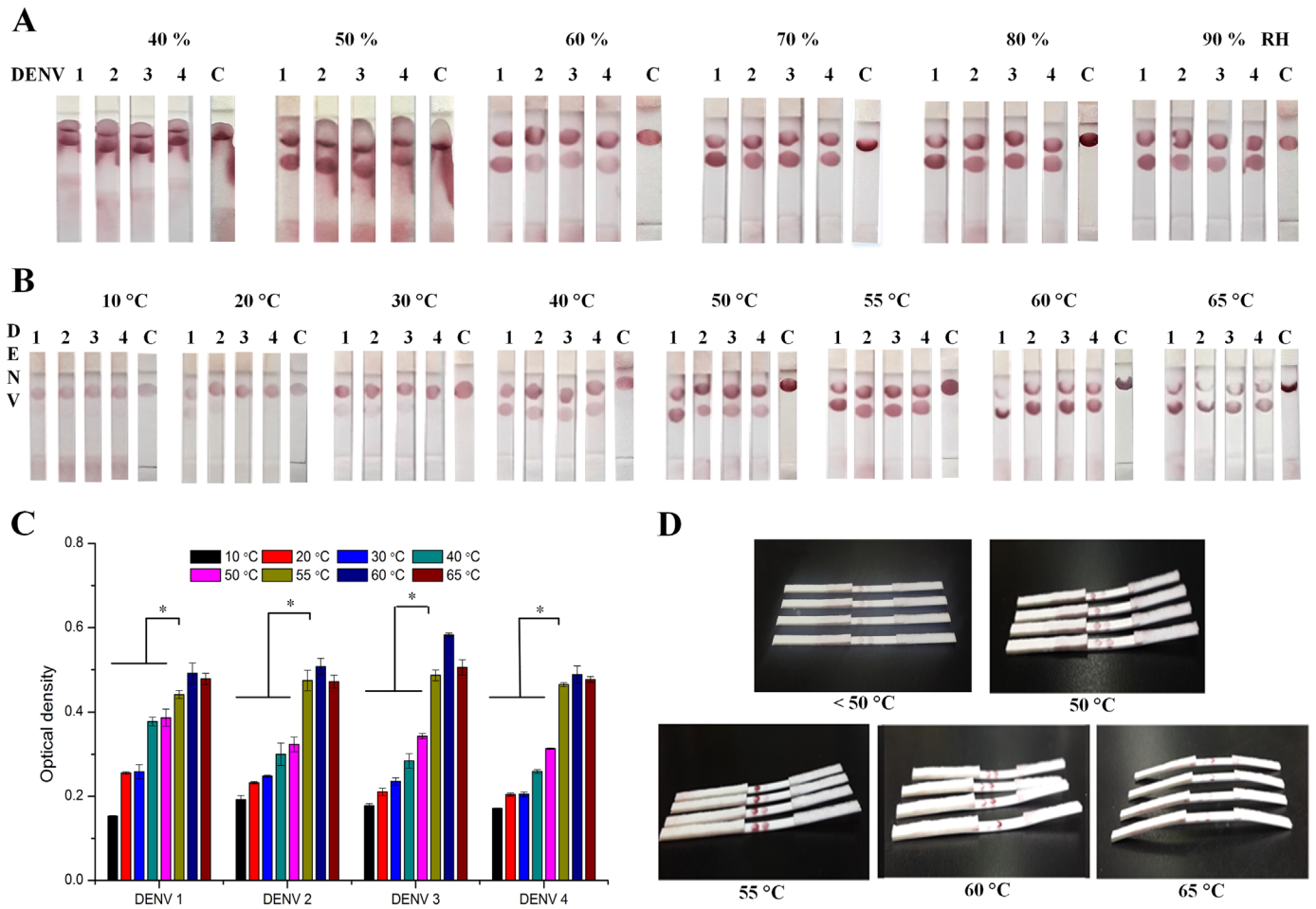

Fig. 3. Temperature and humidity effects on nucleic acid-based lateral flow assay. (A) Humidity affects the fluid flow in LFA. We found that at low humidity (40% RH), the fluid was unable to completely diffuse across the nitrocellulose membrane, whereas the RH > 60% enabled the complete fluid diffusion across the nitrocellulose membrane. (B and C) 55–60 °C enhanced the signal of nucleic acid-based LFA (*$p < 0.05$ relative to 55 °C). (D) High temperature (> 50 °C) altered the shape of paper.

increasing the hybridization rate between the capture probe and target DNA. However, increasing the concentration of capture probe from 100 to 500 μM produced no significant difference in optical density (Supplementary Fig. 2A), indicating that maximal hybridization had already occurred at 100 μM. Considering the assay cost and the sensitivity of the assay, 100 μM was selected as the optimum capture probe concentration for the subsequent experiments.

To determine the optimum concentration of AuNP-DP, we performed the assay using 3 nM, 6 nM and 9 nM of AuNP-DP. We found that the optical density of the test zone in LFA was significantly increased by increasing concentration of AuNP-DP ($p < 0.05$) due to the high amount of AuNP-DP available for DNA hybridization. However, 3 nM of AuNP-DP produced less background signal than 6 nM and 9 nM, as indicated by the significant lower optical density of background as compared to that of 6 nM and 9 nM (Supplementary Fig. S2B). The concentration of 3 nM was also found optimum to avoid non-specific adsorption of the excess reagent onto the membrane. Given that a high background signal might affect the assay readout, we chose 3 nM of AuNP-DP for subsequent experiments.

To determine the optimum concentration of SSC buffer, which promotes DNA hybridization, we performed the assay using 2 ×, 4 ×, 6 × and 8 × SSC buffer. We found that higher concentrations of SSC buffer significantly increased the optical density of the test zone in LFA ($p < 0.05$). However, 2 × and 4 × of SSC buffer showed a significantly lower background signal as compared to that of 6 × and 8 × (Supplementary Fig. S2C). Therefore, 4 × of SSC buffer was selected for subsequent assays, which produced a clearly visible test zone and a low background signal, compared to the other concentrations tested.

With the optimum concentration of capture probe, AuNP-DP and SSC buffer, sensitivity and specificity assays were performed under ambient condition. The test strip was able to achieve a detection limit of as low as 5–10 nM, as indicated by the detection limit of as low as 5 nM achieved for DENV 1, 2 and 4, and the detection limit of 10 nM achieved for DENV 3 (Fig. 2A and B). The assay was highly specific, as evidenced by the negative result shown in the presence of HIV, plasmodium sp. and SSC buffer. A positive result was shown only in the presence of DENV (Fig. 2C).

3.3. Effect of temperature and RH on DNA hybridization

To achieve an optimum DNA hybridization on the test strip without changing the shape of paper which might in turn disrupt the fluid diffusion across the paper, we manipulated two main environmental factors (i.e., temperature and RH) in the assay. The test strip was initially tested over a range of 40–90% RH. RH represents the ratio of the partial pressure of water vapour to its saturation vapour pressure at particular temperature. We found that at low humidity, particularly at 40% RH, the fluid was unable to completely diffuse across the nitrocellulose membrane, whereas RH > 60% enabled the fluid to completely diffuse across the nitrocellulose membrane (Fig. 3A). This might be due to water evaporation at low RH. The

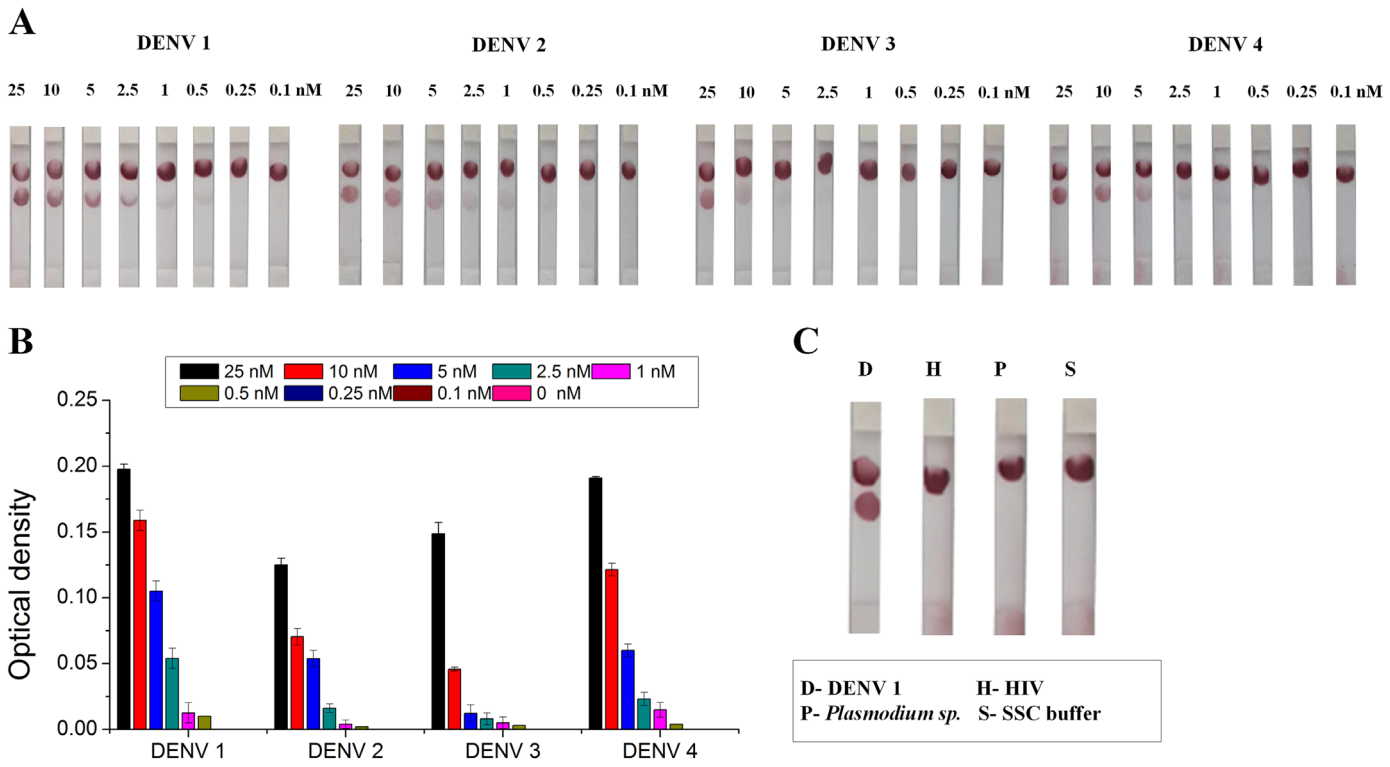

Fig. 4. Sensitivity and specificity assay at optimum temperature and RH. (A and B) The detection limit of the asssay at optimum condition was as low as 0.5–2.5 nM, as indicated by the detection limit of as low as 0.5 nM achieved by DENV 1, 2 and 4, and 2.5 nM achieved by DENV 3. (C) The assay is highly specific as indicated by the only positive result shown in the presence of DENV.

phenomenon can be explained by the equation, ($M_{ev}=(1-RH)\times P_w\times(0.089+0.0782\,V_a)/\gamma$), where M_{ev}, P_w, V_a and γ are the evaporation rate, the water saturated pressure, the air flow rate and the latent heat of vaporization of water, respectively. Theoretically, in a closed system, with a fixed temperature, the air flow rate is assumed to be zero, whereas the water saturated pressure and the latent heat of vaporization of water remain constant (Liu et al., 2014). In this case, the evaporation rate is directly proportional to the (1-RH). This equation supports our experimental data, indicating that the higher the RH, the lower the evaporation rate. In agreement with this principle, our data showed that low environmental RH led to the water loss from the test strip via evaporation, as indicated by the lower weight of test strip (Data not shown), which ultimately reduced the wicking rate of the fluid. The reduction of fluid wicking rate resulted in the accumulation of free AuNP-DP and AuNP-DP-target DNA along the nitrocellulose membrane, thus producing a false positive result (Fig. 3A). On the contrary, RH beyond 60% reduced the water evaporation. As a result, the fluid was able to completely diffuse across the nitrocellulose membrane and yielded the desired signal.

With the average optimum RH (80%), we further tested the test strip over a range of environmental temperatures (10, 20, 30, 40, 50, 55, 60, 65, 70, 80 and 90 °C). We found that the intensity of the test zone increases with increasing temperature, until 65 °C. A temperature of 55–60 °C shows the greatest DNA hybridization effect, as evidenced by the high colour intensity of the test zone and the high value of optical density ($p<0.05$) (Fig. 3B and C). A temperature of 55 °C, in particular, showed the most visible colour at both control and test zones. However, the signal reduced with further increase of temperature (>65 °C), which represents the melting point of the primers. This can be fully supported by the principle of PCR, which shows that 55 °C is an optimum annealing temperature (Jia et al., 2014; Reske et al., 2007; Vlachou et al., 2010). At low temperature (<55 °C), the molecular kinetics are low and most DNA remains double-stranded (Lander et al., 2012; Sorgenfrei et al., 2011). However, as temperature increases, molecular kinetics (i.e., molecular motion) increases, which induces more frequent collisions between single-stranded DNA and primers, resulting in a higher reaction rate and thus more double-stranded DNAs (Lander et al., 2012; Sorgenfrei et al., 2011). When the temperature gets closer to the melting point of the target DNA (~65 °C), the double-stranded DNA starts to dissociate, thus reducing the hybridization signal. Additionally, we observed that starting from 50 °C, the test strip was slightly deformed (Fig. 3D). Surprisingly, we found that at 70 °C, the components of the test strip started to fall apart (Data not shown), mainly because of the non-homogenous thermally-induced deformation of different component of the test strip (due to the different coefficients of thermal expansion). The thermal expansion coefficient of glass fiber, cellulose, nitrocellulose membrane and polyvinylchloride are approximately 12, 2, 30 and 28 ($\times 10^{-6}$ in/in °F) respectively. The mismatch between the coefficient of thermal expansion of different materials caused the test strip to be susceptible to deformation with large temperature change (Okahisa et al., 2009). The deformation of backing pad, which serves as a support, caused a slight detachment of immersing pad, thus disallowing the fluid flow to the nitrocellulose membrane, and eventually producing no result. This phenomenon suggests that temperature may markedly affect the properties and the shape of paper, and thus negatively influence the outcome of LFA. Further, the sensitivity and specificity assays were performed at optimum condition (55 °C, 80% RH). We found that the test strip was able to achieve a detection limit of as low as 0.5–2.5 nM (0.5 nM achieved by DENV 1, 2 and 4, and 2.5 nM achieved by DENV 3), which is almost 10-fold lower than that achieved under ambient conditions (5–10 nM) (25 °C, 60% RH) (Fig. 4A and B). In addition, the assay was highly specific at optimum conditions as witnessed by the positive result shown only in the presence of target DENV (Fig. 4C).

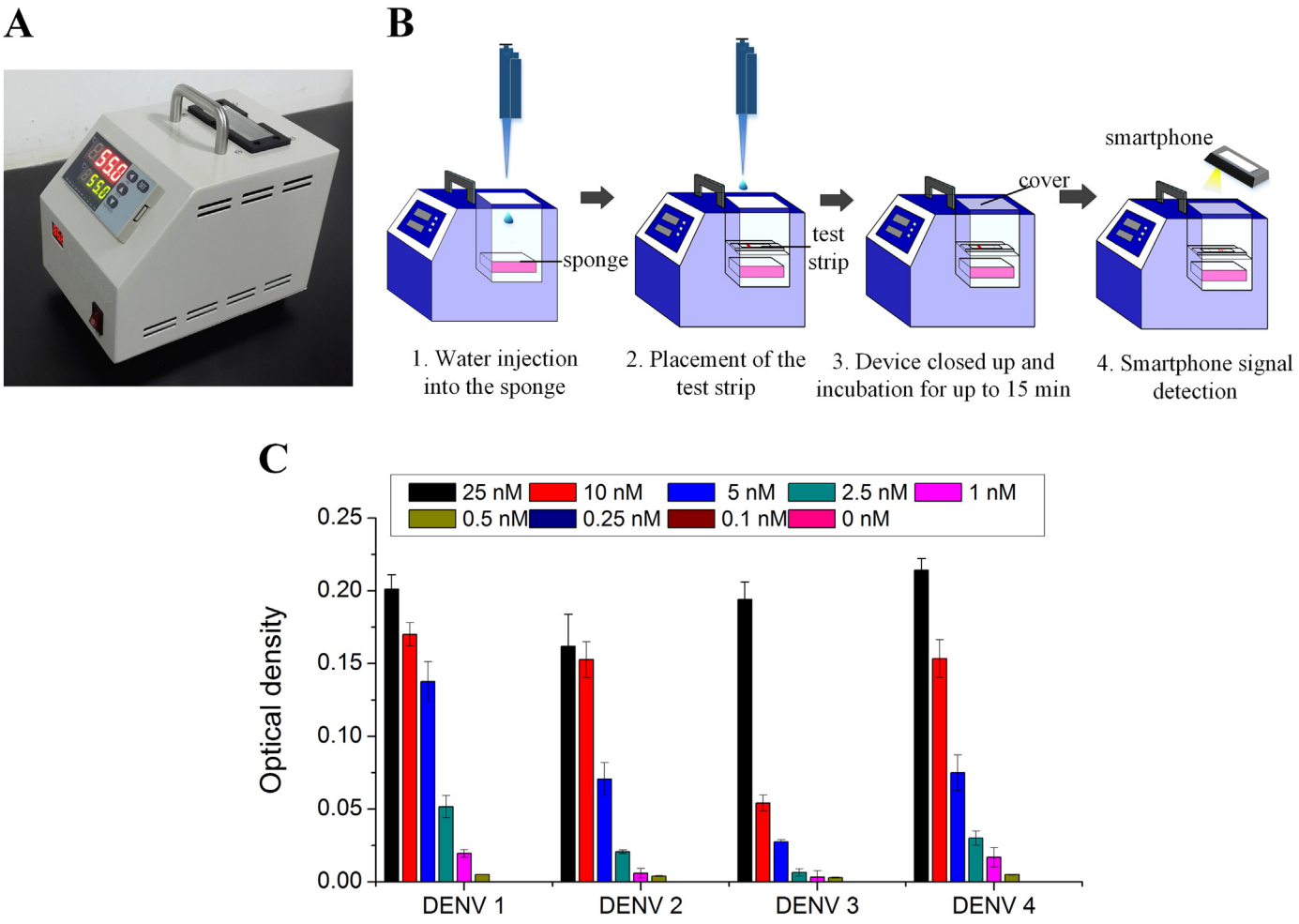

Fig. 5. Portable temperature–humidity control device for DENV DNA detection. (A) A photo image of the device. (B) The schematic diagram of experimental procedure. In line with the data of temperature–humidity control device, by using this portable device, the detection limit for nucleic acid detection could reach as low as 0.5–2.5 nM (C), representing 10-fold enhancement.

3.4. A portable temperature–humidity control device designed for target analyte detection

To enable accurate diagnosis of infectious diseases in resource-limited settings with extreme temperature or humidity, development of a portable and affordable diagnostic technique is crucial. Therefore, we developed a portable temperature–humidity control device specifically designed for LFA for effective target detection in low resource settings (Fig. 5A). Generally, the device consists of a testing compartment, an integrated battery, an integrated temperature controller, a sponge and a charger. This closed device is internally made of a good thermal conductor, aluminium alloy, with external insulation wall, with a glass window on top for visual signal detection or detection by a smartphone. A range of temperatures (25–100 °C) can be achieved with an accuracy of ± 0.1 °C by direct current produced by a battery power source integrated into the device, to maintain the optimum performance of this portable device. The test strip is placed right below the glass, supported by an aluminium supporting frame at the middle layer of the compartment, whereas the bottom layer of the compartment consists of a damp sponge, which sustains the humidity of the compartment. In addition, temperature and humidity sensors are installed in the internal part of the device, with a thermo-hygrometer placed at the exterior part to ensure the maintenance of temperature and RH over 30 min. Briefly, water is injected into the sponge to achieve the desired RH of the compartment at the desired temperature (Fig. 5B). Following the addition of sample, the testing compartment is closed for LFA for 10–15 min. In line with the data produced by temperature–humidity control chamber, this simple and portable device allows sensitive detection of the DNA of DENV.

To verify the effect of temperature and humidity on nucleic acid hybridization in LFA, we further tested the test strip with another model analyte, the DNA of HIV using our small device. Similar to DENV, a temperature of 55–60 °C showed the greatest DNA hybridization, as indicated by the significantly highest colour intensity of test zone and the highest OD value ($p < 0.05$) (Fig. 6A). The data strongly suggests that the proof-of-principle of the annealing process in PCR can be successfully achieved by using a test strip, with dependence on temperature and RH.

In addition, to further prove the ability of paper-based assays to support the theory of temperature effect, we selected an Ag (C-reactive protein) as a model of the assay. We observed that among all temperatures, 37–40 °C produced the highest signal ($p < 0.05$) (Fig. 6B), with a detection limit of 1 ng/ml, which is lower than the 2.5 ng/ml observed at ambient temperature (Fig. 6C). Our data showed the highest optical density of the test zone at 37 °C ($p < 0.05$), indicating the highest number of Ag–Ab reactions, which is in agreement with the existing theory (Reverberi and Reverberi, 2007). Theoretically, given that at 37–40 °C, the strength of the bonding between Ag and Ab are the most stable among various temperature (Reverberi and Reverberi, 2007). This binding occurs preferentially at low temperature and may start to dissociate at higher temperature (England and Haran, 2011). A

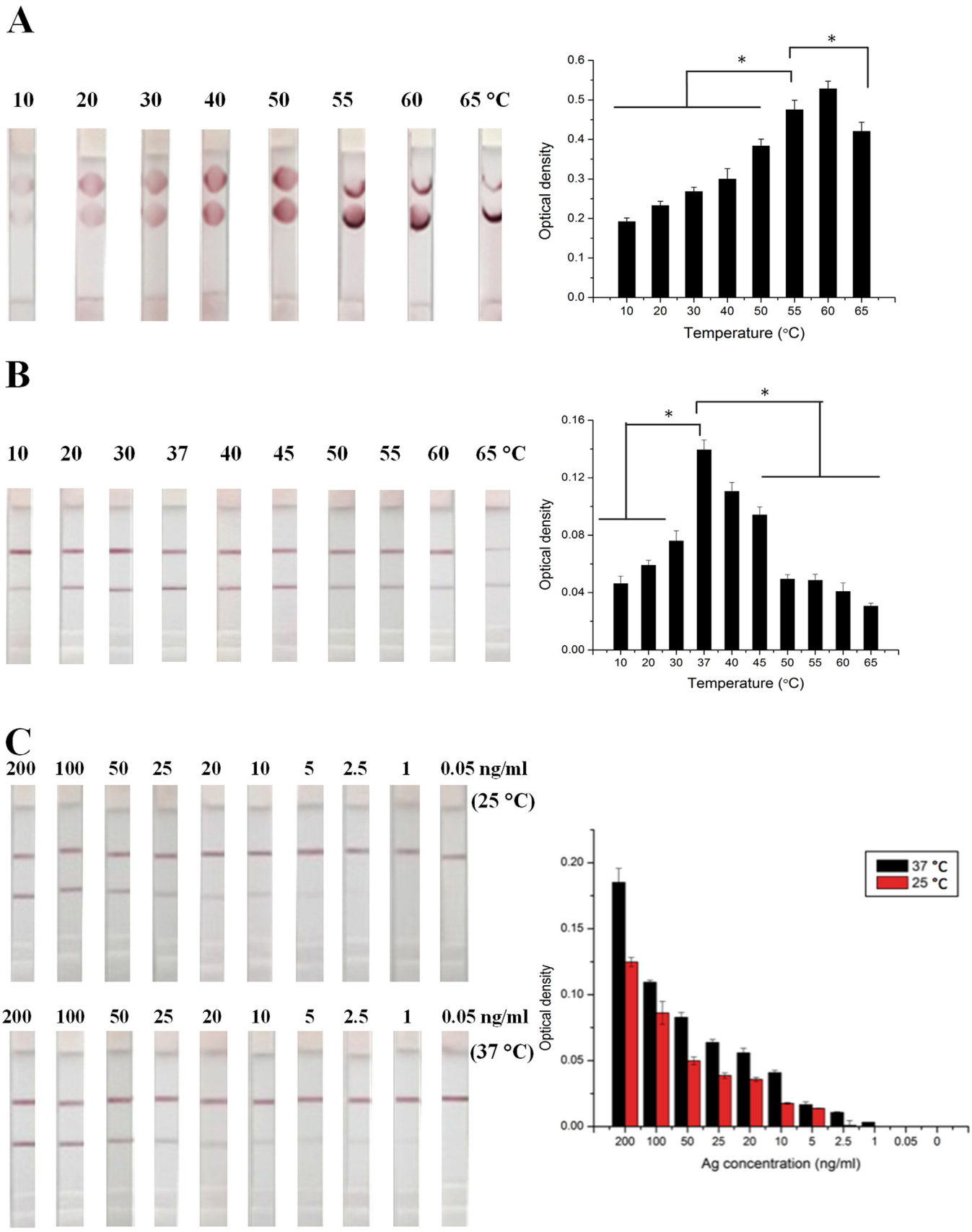

Fig. 6. HIV DNA and C-reactive protein detection using temperature–humidity control device. (A) Temperature of 55–60 °C showed the greatest signal of nucleic acid-based LFA in HIV DNA detection (*$p < 0.05$ relative to 55 °C). (B) 37–40 °C produced the greatest signal in C-reactive protein detection (*$p < 0.05$ relative to 37 °C), with a lower detection limit (1 ng/ml) than that achieved at ambient temperature (2.5 ng/ml), representing 3-fold signal enhancement (C).

temperature of <30 °C showed a weaker reaction, while a temperature beyond 45 °C showed extremely weak or no reaction, which might be due to the protein denaturation and changes in antigenic structures. Taken together, the portable device was able to improve the sensitivity of LFA in nucleic acid and antigen detection with the optimum RH of 70–90% and temperatures of 55–60 °C and 37–40 °C, respectively.

Even though the optimum temperatures of 55–60 °C and 37–40 °C obtained from the present study represent the well-known optimum temperatures for nucleic acid hybridization and antigen–antibody interaction, respectively, we are the first group to demonstrate the potential of the test strip to allow effective biomolecular interactions at these optimum temperatures. In addition to temperature, the appropriate relative humidity (RH) ($>60\%$) for LFAs is also suggested. With the introduction of a portable temperature–humidity control device, our finding is not only useful to provide better understanding of the significance of environmental conditions for effective biomolecular interaction on paper, but also provides an idea of significantly enhancing the sensitivity of the assay in a portable manner.

We envision that in the future, the integration of paper-based sample-to-answer biosensor into this portable device could sensitively detect various targets with only single drop of blood. For example, in nucleic acid testing, the integrated paper-based nucleic acid extraction and selected isothermal amplification (e.g. nucleic acid sequence-based amplification (NASBA) or strand displacement amplification (SDA)) could produce single-stranded RNA or DNA, which could in turn hybridize with the complementary probe on the test zone and eventually produce a colorimetric signal. With the advanced fluidic control technologies in paper (e.g. paper-based valves), the flow of the sample from one functional zone to another (e.g. from amplification zone to detection zone) could be precisely controlled in this integrated biosensor. The portable temperature–humidity control device permits the sequentially shifts between the desired temperatures and remains at each temperatures for a specified length of time. Therefore, it allows pre-setting of the temperature and time required for each step of extraction, amplification and sensitive detection. As for the antigen detection, a blood separator (e.g., fusion 5) could be integrated into the test strip for whole blood separation. The serum containing the target antigen would then wick through the nitrocellulose membrane and bind to the antibody on the test zone, which could eventually produce an enhanced colorimetric signal by using this portable device.

4. Conclusion

In short, with the simple temperature–humidity control device, we successfully proved that temperatures of 55–65 °C and 37–40 °C, with a humidity of 70–90% give an optimum signal for nucleic acid and antigen detection in LFA respectively. This compact, portable and cost-effective temperature–humidity control model, coupled with the test strip, offers rapid, specific and sensitive diagnosis of infectious diseases in POC settings. We expect that our prototype will raise concerns about the significance of the impact of environmental monitoring on biomolecular reactions in LFA, which could maximize the usage of paper-based material in biomedical areas. We envision that integration of paper-based sample-to-answer biosensor into the portable device coupled with signal detection by a smartphone (Xu et al., 2015) could rapidly, accurately and sensitively detect a variety of target analytes (nucleic acid, Ag or Ab) in remote settings.

Acknowledgement

This work was financially supported by the Major International Joint Research Program of China (11120101002), the International Science & Technology Cooperation Program of China (2013DFG02930), and the Ministry of Higher Education (MOHE), Government of Malaysia under the high impact research (UM.C/HIR/MOHE/ENG/44). FX was partially supported by the China Young 1000-Talent Program and Program for New Century Excellent Talents in University (NCET-12-0437). The work was performed at Bioinspired Engineering and Biomechanics Center (BEBC) at Xi'an Jiaotong University. All authors declare no conflict of interest.

Appendix A. Supplementary material

Supplementary data associated with this article can be found in the online version at http://dx.doi.org/10.1016/j.bios.2015.12.005.

References

Barry, J.F., DeMille, D., 2012. Low-temperature physics: a chilling effect for molecules. Nature 491 (7425), 539–540.
Blažková, M., Koets, M., Rauch, P., van Amerongen, A., 2009. Development of a nucleic acid lateral flow immunoassay for simultaneous detection of Listeria spp. and Listeria monocytogenes in food. Eur. Food Res. Technol. 229 (6), 867–874.
Burke, A.M., Gorodetsky, A.A., 2012. Electrochemical sensors: taking charge of detection. Nat. Chem. 4 (8), 595–597.
Cate, D.M., Adkins, J.A., Mettakoonpitak, J., Henry, C.S., 2014. Recent developments in paper-based microfluidic devices. Anal. Chem. 87 (1), 19–41.
Chien, L.J., Liao, T.L., Shu, P.Y., Huang, J.H., Gubler, D.J., Chang, G.J., 2006. Development of real-time reverse transcriptase PCR assays to detect and serotype dengue viruses. J. Clin. Microbiol. 44 (4), 1295–1304.
Choi, J.R., Tang, R., Wang, S., Abas, W.A.B.W., Pingguan-Murphy, B., Xu, F., 2015. Paper-based sample-to-answer molecular diagnostic platform for point-of-care diagnostics. Biosens. Bioelectron. 74, 427–439.
Dauner, A.L., Mitra, I., Gilliland Jr, T., Seales, S., Pal, S., Yang, S.-C., Guevara, C., Chen, J.-H., Liu, Y.-C., Kochel, T.J., Wu, S.-J.L., 2015. Development of a pan-serotype reverse transcription loop-mediated isothermal amplification assay for the detection of dengue virus. Diagn. Microbiol. Infect. Dis. 83 (1), 30–36.
De Roy, K., Marzorati, M., Negroni, A., Thas, O., Balloi, A., Fava, F., Verstraete, W., Daffonchio, D., Boon, N., 2013. Environmental conditions and community evenness determine the outcome of biological invasion. Nat. Commun. 4, 1383.
England, J.L., Haran, G., 2011. Role of solvation effects in protein denaturation: from thermodynamics to single molecules and back. Annu. Rev. Phys. Chem. 62, 257.
Feng, S., Choi, J.R., Lu, T.J., Xu, F., 2015. State-of-art advances in liquid penetration theory and flow control in paper for paper-based diagnosis. Adv Porous Flow. 5, 16–29.
Giokas, D.L., Tsogas, G.Z., Vlessidis, A.G., 2014. Programming fluid transport in paper-based microfluidic devices using razor-crafted open channels. Anal. Chem. 86 (13), 6202–6207.
Han, Y.L., Hu, J., Genin, G.M., Lu, T.J., Xu, F., 2014. BioPen: direct writing of functional materials at the point of care. Sci. Rep. 4, 4872–4876.
He, Y., Zhang, S., Zhang, X., Baloda, M., Gurung, A.S., Xu, H., Zhang, X., Liu, G., 2011. Ultrasensitive nucleic acid biosensor based on enzyme–gold nanoparticle dual label and lateral flow strip biosensor. Biosens. Bioelectron. 26 (5), 2018–2024.
Hu, J., Wang, L., Li, F., Han, Y.L., Lin, M., Lu, T.J., Xu, F., 2013. Oligonucleotide-linked gold nanoparticle aggregates for enhanced sensitivity in lateral flow assays. Lab. Chip 13 (22), 4352–4357.
Hu, J., Wang, S., Wang, L., Li, F., Pingguan-Murphy, B., Lu, T.J., Xu, F., 2014. Advances in paper-based point-of-care diagnostics. Biosens. Bioelectron. 54 (0), 585–597.
Jia, H., Guo, Y., Zhao, W., Wang, K., 2014. Long-range PCR in next-generation sequencing: comparison of six enzymes and evaluation on the MiSeq sequencer. Sci. Rep. 4, Article No. 5737.
Johnson, B.W., Russell, B.J., Lanciotti, R.S., 2005. Serotype-specific detection of dengue viruses in a fourplex real-time reverse transcriptase PCR assay. J. Clin. Microbiol. 43 (10), 4977–4983.
Lander, B., Seifert, U., Speck, T., 2012. Effective confinement as origin of the equivalence of kinetic temperature and fluctuation-dissipation ratio in a dense shear-driven suspension. Phys. Rev. E 85 (2), 021103.
Laursen, L., 2012. Point-of-care tests poised to alter course of HIV treatment. Nat. Med. 18 (8) 1156.
Liu, Z., Hu, J., Zhao, Y., Qu, Z., Xu, F., 2015. Experimental and numerical studies on liquid wicking into filter papers for paper-based diagnostics. Appl. Therm. Eng. 88, 280–287.

Lutz, B., Liang, T., Fu, E., Ramachandran, S., Kauffman, P., Yager, P., 2013. Dissolvable fluidic time delays for programming multi-step assays in instrument-free paper diagnostics. Lab. Chip 13 (14), 2840–2847.
Martinez, A.W., 2011. Microfluidic paper-based analytical devices: from POCKET to paper-based ELISA. Bioanalysis 3 (23), 2589–2592.
McNerney, R., Daley, P., 2011. Towards a point-of-care test for active tuberculosis: obstacles and opportunities. Nat. Rev. Microbiol. 9 (3), 204–213.
Mudanyali, O., Dimitrov, S., Sikora, U., Padmanabhan, S., Navruz, I., Ozcan, A., 2012. Integrated rapid-diagnostic-test reader platform on a cellphone. Lab. Chip 12 (15), 2678–2686.
Okahisa, Y., Yoshida, A., Miyaguchi, S., Yano, H., 2009. Optically transparent wood–cellulose nanocomposite as a base substrate for flexible organic light-emitting diode displays. Compos. Sci. Technol. 69 (11), 1958–1961.
Parolo, C., Medina-Sanchez, M., de la Escosura-Muniz, A., Merkoci, A., 2013. Simple paper architecture modifications lead to enhanced sensitivity in nanoparticle based lateral flow immunoassays. Lab. Chip 13 (3), 386–390.
Qin, Z., Chan, W.C., Boulware, D.R., Akkin, T., Butler, E.K., Bischof, J.C., 2012. Significantly improved analytical sensitivity of lateral flow immunoassays by using thermal contrast. Angew. Chem. Int. Ed. Engl. 51 (18), 4358–4361.
Renault, C., Li, X., Fosdick, S.E., Crooks, R.M., 2013. Hollow-channel paper analytical devices. Anal. Chem. 85 (16), 7976–7979.
Reske, T., Mix, M., Bahl, H., Flechsig, G.-U., 2007. Electrochemical detection of osmium tetroxide-labeled PCR-products by means of protective strands. Talanta 74 (3), 393–397.
Reverberi, R., Reverberi, L., 2007. Factors affecting the antigen-antibody reaction. Blood Transfus. 5 (4), 227.
Rivas, L., Medina-Sánchez, M., de la Escosura-Muñiz, A., Merkoçi, A., 2014. Improving sensitivity of gold nanoparticle-based lateral flow assays by using wax-printed pillars as delay barriers of microfluidics. Lab. Chip 14 (22), 4406–4414.
Sackmann, E.K., Fulton, A.L., Beebe, D.J., 2014. The present and future role of microfluidics in biomedical research. Nature 507 (7491), 181–189.
Song, Y., Zhang, Y., Bernard, P.E., Reuben, J.M., Ueno, N.T., Arlinghaus, R.B., Zu, Y., Qin, L., 2012. Multiplexed volumetric bar-chart chip for point-of-care diagnostics. Nat. Commun. 3, 1283.
Sorgenfrei, S., Chiu, C.-y, Gonzalez, R.L., Yu, Y.-J., Kim, P., Nuckolls, C., Shepard, K.L., 2011. Label-free single-molecule detection of DNA-hybridization kinetics with a carbon nanotube field-effect transistor. Nat. Nano 6 (2), 126–132.
Stubbs, S.L., Hsiao, S.T.-F., Peshavariya, H.M., Lim, S.Y., Dusting, G.J., Dilley, R.J., 2011. Hypoxic preconditioning enhances survival of human adipose-derived stem cells and conditions endothelial cells in vitro. Stem Cells Dev. 21 (11), 1887–1896.
Teoh, B.T., Sam, S.S., Tan, K.K., Danlami, M.B., Shu, M.H., Johari, J., Hooi, P.S., Brooks, D., Piepenburg, O., Nentwich, O., Wilder-Smith, A., Franco, L., Tenorio, A., AbuBakar, S., 2015. Early detection of dengue virus by use of reverse transcription-recombinase polymerase amplification. J. Clin. Microbiol. 53 (3), 830–837.
Vlachou, M.A., Glynou, K.M., Ioannou, P.C., Christopoulos, T.K., Vartholomatos, G., 2010. Development of a three-biosensor panel for the visual detection of thrombophilia-associated mutations. Biosens. Bioelectron. 26 (1), 228–234.
Wang, C., Zhang, L., Shen, X., 2013. Development of a nucleic acid lateral flow strip for detection of hepatitis C virus (HCV) core antigen. Nucleosides, Nucleotides Nucleic Acids 32 (2), 59–68.
Wu, G., Srivastava, J., Zaman, M.H., 2014. Stability measurements of antibodies stored on paper. Anal. Biochem. 449 (0), 147–154.
Xu, X., Akay, A., Wei, H., Wang, S., Pingguan-Murphy, B., Erlandsson, B.-E., Li, X., Lee, W., Hu, J., Wang, L., 2015. Advances in smartphone-based point-of-care diagnostics. Proc. IEEE 103 (2), 236–247.
Zhang, D.Y., Chen, S.X., Yin, P., 2012. Optimizing the specificity of nucleic acid hybridization. Nat. Chem. 4 (3), 208–214.